Fish and Shellfish Immunology 92 (2019) 861–870

Contents lists available at ScienceDirect

Fish and Shellfish Immunology

journal homepage: www.elsevier.com/locate/fsi

Full length article

Evolutionary adaptation analysis of immune defense and hypoxia tolerance in two closely related *Marsupenaeus* species based on comparative transcriptomics

Panpan Wang[a], Chaofan Xing[b], Jun Wang[a], Yongquan Su[a], Yong Mao[a,*]

[a] State Key Laboratory of Marine Environmental Science, College of Ocean and Earth Sciences, Xiamen University, Xiamen, 361102, Fujian, China
[b] State Key Laboratory of Cellular Stress Biology, School of Life Sciences, Xiamen University, Xiamen, 361102, Fujian, China

ARTICLE INFO

Keywords:
Adaptive evolution
Marsupenaeus japonicus
Marsupenaeus pulchricaudatus
Immune defense
Hypoxia tolerance
Transcriptomics

ABSTRACT

Kuruma shrimp, a major farmed shrimp species in the world, includes two cryptic or sibling species, Form I (*Marsupenaeus japonicus*) and Form II (*Marsupenaeus pulchricaudatus*). Due to the lack of genomic resources, little is known about the molecular mechanisms associated with immune defense and hypoxia tolerance. Here, we sequenced the transcriptomes of two closely related *Marsupenaeus* species and compared genomic divergence. This study obtained 77049 and 84561 unigenes with N50 values of 1281bp and 1244bp for *M. japonicus* and *M. pulchricaudatus*, respectively, and 5036 pairs of putative orthologs were identified between two *Marsupenaeus* species. Estimation of *Ka/Ks* ratios indicated that 165 orthologous genes may be under positive selection (*Ka/Ks* > 0.5), including 49 pairs with a *Ka/Ks* ratio > 1. According to the peak of synonymous rates, the divergence time between *M. japonicus* and *M. pulchricaudatus* was about 0.26–0.69 Mya. These positively selected orthologous genes related to the immune process mainly comprised single *VWC* domain protein, *legumain*, *ras-related C3* botulinum, *caspase*, *C-type lectin* and were enriched in functions related to immune (Toll-like receptor and PI3K-Akt signaling) and hypoxia signaling (HIF-1 signaling and VEGF signaling). In this study, dozens of caspase-like unigenes were screened from two *Marsupenaeus* transcriptomes. Among these, the *PjCaspase* orthologous gene was subjected to positive selection (*Ka/Ks* = 1.22), which had different secondary and three-dimensional structure prediction. Based on the single copy caspase gene, eight populations of *Marsupenaeus* species were divided into two phylogeographic lineages from the East and South China. We characterized the transcriptomes of the two *Marsupenaeus* species and obtained several key orthologs associated with immune defense and hypoxia tolerance, which provides new insights into the immunity and genetic divergence of the two varieties. Moreover, this study will facilitate further comparative genomic studies of the two varieties.

1. Introduction

The kuruma shrimp *Marsupenaeus japonicus* (Decapoda, Penaeidae, *Marsupenaeus*) is recognized as one of the main farmed shrimp groups in the world and is widely distributed in the East China Sea, the South China Sea, the region off Australia and the western Indian Ocean [1,2]. *M. japonicus* has been regarded as the only morphological species of *Marsupenaeus* [3,4]. In a study by Tsoi et al. [5], two morphologically similar varieties, I and II, were characterized by their carapace color banding patterns, indicating the occurrence of cryptic species. Forms I was confined to the northern South China Sea and the East China Sea (including Japan), while forms II consisted of populations from the South China sea, Southeast Asia and Australia [6]. These two units are distributed mostly allopatrically but overlap in the northern coasts of the South China Sea and Taiwan [6,7]. Subsequently, Tsoi et al. revised their taxonomic status and named the species *Marsupenaeus japonicus* (Form I) and *Marsupenaeus pulchricaudatus* (Form II) [2]. However, thus far, almost all studies about kuruma shrimp population structure analysis have been based on mitochondrial sequences and ribosomal DNA. The mitochondrial sequences follow maternal inheritance and paternal leakage [8], which could not provide direct evidence for hybrids. The ribosomal DNA possess multiple copies and is easy to be homogenized. The SCNGs (Single-copy nuclear genes) contain rich genetic information from parents, which can better reflect the evolutionary history of species then mitochondrial DNA [9,10]. In addition, norms and methods for species delimitation are improving, and it is difficult to accurately discover cryptic diversity based on existing genetic data [11–14].

* Corresponding author.
E-mail address: maoyong@xmu.edu.cn (Y. Mao).

https://doi.org/10.1016/j.fsi.2019.06.055
Received 26 February 2019; Received in revised form 22 June 2019; Accepted 29 June 2019
Available online 02 July 2019

Although the two varieties have only subtle morphological differences, they have different advantages related to growth [15] and thermotolerance [16]. Some incoherent records about the environmental conditions required by the kuruma shrimp from various regions were summarized [2]. The kuruma shrimp aquaculture is widespread and failure of culture is still being occasionally reported, which may due to obscure source of the shrimps and inadequate immunopathogenesis studies. At present, shrimp diseases (viruses, bacteria and parasites) and environment degradation are two serious challenges faced by shrimp farming in the word. As invertebrates, crustaceans mainly rely on the innate immune system [17]. Hepatopancreas, a multifunctional organ, integrate immune functions and metabolism [18]. The hepatopancreas is an important source of molecules of innate immunity, involving in antigen processing and pathogen clearance [19,20]. Ren et al. [21] sequenced the transcriptomes of *M. japonicus* hepatopancreas in response to *Vibrio parahaemolyticus* and white spot syndrome virus, and obtained several immune-related genes including *caspase 4*, *crustin* and *C-type lectin*. Several studies on immune functions of *M. japonicus* have mainly concentrates on immune-related molecules, such as Toll-like receptor [22], caspase [19,23], C-type lectin [24] and AMPs [25]. However, there are hardly any immune-related studies about *M. pulchricaudatus*. As two closely related *Marsupenaeus* species, all relevant biological studies should be revaluated, especially immune defense function.

Recent rapid developments in next generation sequencing (NGS) have provided data on penaeid species [26–29]. However, nearly all research has focused on differentially expressed transcripts in one species under different conditions and during reproduction or development. Comparative RNA-sequencing between closely related species can offer unprecedented opportunities to study species-specific adaptations and evolutionary origins [30,31]. For instance, Li et al. sequenced the transcriptomes of bighead carp and silver carp, and obtained many important candidate genes related to resistance to environmental stress [32]. Additional studies of comparative RNA-Seq analyses include studies investigating mussels [33], *Cipangopaludina cahayensis* and *Pomacea canaliculata* [34], *Lissotriton boscai* [35], and *Calanus finmarchicus* and *Calanus glacialis* [36]. Considering the status of *M. japonicus* studies, little is known about the molecular mechanisms associated with adaptational abilities and the evolutionary adaptation of immune defense functions, largely due to the lack of sufficient genetic or genomic information.

To comprehensively comprehend the molecular mechanisms underlying genetic differentiation and explore the evolutionary processes, a comparative transcriptomic analysis was first performed on hepatopancreas tissues from *M. japonicus* and *M. pulchricaudatus*. This study provides abundant transcriptome resources and new insights into the genetic divergence and evolutionary adaptation of immune defense functions of the two varieties, and also provides a better understanding of the differences in resistance to some pathogens.

2. Materials and methods

2.1. Sample collection and RNA extraction

All *M. japonicus* prawns (16–25 individuals per site) were sampled from eight locations along the southeast coast of China, including Zhoushan (ZS), Xiapu (XP), Xiamen (XM), Huilai (HL), Zhuhai (ZH), Dongdi (DD), Qiaogang (QG) and Sanya (SY) (Fig. S1). Animal treatment was conducted in strict accordance with the recommendations of Animal Care Quality Assurance in China. The body length, body weight, gender and carapace banding patterns of all individuals were recorded. Part of the abdominal muscle was preserved in 95% ethanol for subsequent DNA extraction. Genomic DNA was extracted using Marine Animals DNA kit (Tiangen, China) for subsequent analysis.

The hepatopancreas tissues of ten healthy *M. japonicus* (HL1, weight: 12.67 ± 3.22 g) and ten healthy *M. pulchricaudatus* (HL2, weight: 11.36 ± 4.2 g) from Huilai (Guangdong, China) were rinsed separately with RNase-free water for transcriptome analysis. In addition, these twenty individuals' genomic DNA were amplified by PCR using *cytochrome b* primers (cytb-f: caaattgttactgggctctttttagct and cytb-r: cagttagcattacgataaatccggt) to ensure sample types (Fig. S2). The total RNA was isolated using RNAiso Plus (TaKaRa, China) from each individual and mixed in equal parts separately. Subsequently, RNA degradation and contamination were monitored by 1% agarose gel electrophoresis. The RNA purity and concentration were measured using a NanoPhotometer® spectrophotometer (IMPLEN, CA, USA). Meanwhile, the RNA integrity was assessed by an RNA Nano 6000 Assay Kit on an Agilent Bioanalyzer 2100 system (Agilent Technologies, CA, USA).

2.2. Library construction and sequencing

For the RNA pool, approximately 3 μg was obtained from each variety following the verification of the RNA integrity using an Agilent 2100 Bioanalyzer (RIN ≥ 8) (Agilent Technologies, USA). Subsequently, mRNA was isolated from total RNA using poly (dT) oligo-attached magnetic beads. The first- and second-strand cDNA was synthesized, and the sequencing libraries were generated using a TruSeq™ RNA Sample Preparation Kit (Illumina, USA) according to the manufacturer's recommendations. The cDNA libraries of the two *Marsupenaeus* species were then sequenced on the Illumina HiSeq X-Ten platform with 150-bp paired-end reads at the Novogene Bioinformatics Technology Co., Ltd. (Beijing, China).

2.3. Sequence assembly and functional annotation

Raw reads in fastq format were first preprocessed by eliminating adaptor sequences and low-quality reads following an assessment by FastQC (http://www.bioinformatics.babraham.ac.uk/projects/fastqc/). The high-quality cleaned reads of the two varieties were separately assembled de novo using the Trinity program with the default parameters [37]. The assembled unigenes were annotated using NCBI BLAST 2.2.28 + and Diamond (v0.8.22) against the Nr, Nt, and Swiss-Prot databases (E-value < $1e^{-5}$), and the euKaryotic Orthologous Groups of proteins (KOG) (E-value < $1e^{-3}$). Unigenes were matched to the Pfam database by Hmmscan 3.0 (E-value = 0.01) [38]. Blast2GO v 2.5 [39] was used to obtain GO annotations based on the results from the Nr and Pfam protein databases (E-value < $1e^{-6}$). Pathway annotations were obtained by utilizing the KAAS program against the KEGG database (E-value < $1e^{-10}$) [40].

2.4. Protein-coding sequence (CDS) prediction

The obtained unigene sequences were searched against the Nr and Swiss-Prot protein databases with a BLASTX algorithm (E-value < $1e^{-5}$). ESTScan (v 3.0.3) [41] was used to predict the coding sequences (CDSs) of sequences that did not have alignment results. The CDSs extracted from their respective unigenes were translated into amino acid sequences (5'- > 3′) according to the standard codon table. Self-to-self BLASTP search was conducted for all amino acid sequences. Subsequently, full-length CDS sequences were obtained by screening predicted coding sequences from BLASTX according to the procedure used by Wang et al. [42]. The 5′UTR and 3′UTR sequences were predicted based on the CDS and start and stop codons.

2.5. Identification of putative orthologs and calculation of Ka/Ks ratios

Orthologous groups were constructed from the BLASTP results with OrthoMCL [43] based on the Markov Cluster algorithm (mcl) using default settings. Protein sequences, translated from single-copy orthologs, were subsequently aligned using MUSCLE 3.8. The alignment result was optimized by Gblocks_0.91b [44], and translated into nucleotide sequences for the subsequent analysis. Subsequently, for these

orthologous genes, non-synonymous substitution rates (*Ka*) and synonymous substitution rates (*Ks*) were estimated by a maximum-likelihood method using the PAML (Phylogenetic Analysis by Maximum Likelihood) toolkit [45]. More non-synonymous substitutions occurred in these orthologous genes when a rate of $Ka/Ks > 1$, suggesting that these genes evolved under positive selection. These divergent genes have a great significance for speciation. Gene ontology illustrates differences in species sequence evolution based on the Wallenius non-central hypergeometric distribution using GOseq [46]. KOBAS software was used to test the statistical KEGG pathway enrichment of divergent and conserved orthologous groups [47]. Gene expression levels were estimated by RSEM (RNA-Seq by Expectation Maximization) software [42] for each sample. To validate the mRNA-Seq data, the relative expression levels of several unigenes were determined by quantitative real time PCR (qRT-PCR) using elongation factor 1-α (EF1-α) as reference gene (Table S1). Real-time PCR efficiencies were determined using the slopes of standard curves and the $2^{-\triangle\triangle CT}$ method was used to calculate the relative expression levels.

2.6. Immune defense and hypoxia tolerance genes

For aquatic animals, higher temperatures are more likely to cause hypoxia [48]. Hemocyanin is to crustaceans what hemoglobin is to mammals. Apoptosis or programmed cell death (PCD) is important for the development and maintenance of cellular homeostasis [49]. According to the unigenes, we designed primers and obtained the coding sequences of *hifα*, *hcy and Mjcaspase* genes. Based on sequence differences, the restriction endonuclease was screened by DNAMAN 9.0 software. The transmembrane region and signal peptide of *Mjcaspase* gene were located by TMHMM Server 2.0 and SignalP-5.0 server, respectively. The secondary structure was predicted using SOPMA [50], SMART [51] and PROSITE [52]. The 3D structures of unigenes were predicted using the homology modeling by the I-TASSER server [53] and the final models were mapped onto the 3D structure using PyMOL (https://pymol.org/2/).

2.7. Population genetic structure analysis

In the study, we obtained a single-copy orthologous gene, which was annotated as caspase gene (EF079670.1). Combined with the result of Southern blot from Zhi et al. [54], it was confirmed that the gene was single copy nuclear gene. Based on the unigene sequences, we designed a pair of primers to amplify the caspase gene. The PCR products were ligated into pEASY®-T1 cloning vector (TransGen Biotech, China). Six clones of each plate were selected randomly for sequencing in both directions. All the sequences were aligned by Clustalx v2.1. The pairwise genetic distances between eight populations were calculated by MEGA X [55] using Kimura 2-parameter model and the UPGMA phylogenetic trees were constructed based the pairwise genetic distance.

2.8. Key resources table

Resource	Source	Identifier
Chemical		
amino acid		
ethanol		
format		
poly (dT)		
ProteinPeptide		
protein		

Table 1
Summary of the statistics for the transcriptome assembly of *M. japonicus* and *M. pulchricaudatus*.

	M. japonicus	*M. pulchricaudatus*
Total number of raw reads	193629906	187827408
Total number of clean reads	178743828	177323416
Total length of clean reads (bp)	26.80G	26.50G
Total number of unigenes	77049	84561
Mean length of unigenes (bp)	704	695
Median length of unigenes (bp)	339	339
Length range of unigenes (bp)	201–38248	201–38243
N50 value of unigenes (bp)	1281	1244
GC percentage (%)	49.53	48.67
Q20% (%)	94.23	93.87

3. Results

3.1. Transcriptome sequencing and assembly

The Illumina sequencing of the *M. japonicus* and *M. pulchricaudatus* cDNA libraries yielded 193.6 million and 187.8 million 150-bp paired-end raw reads, respectively (Table 1). Following quality trimming, we obtained 178.7 million clean reads with a total length of 26.8 Gb for *M. japonicus* and 177.3 million clean reads with a total length of 26.5 Gb for *M. pulchricaudatus* (Table 1). The de novo assembly of the obtained clean reads generated 77049 unigenes with an N50 value of 1281 bp for *M. japonicus* and 84561 unigenes with an N50 value of 1244 bp for *M. pulchricaudatus* (Table 1).

3.2. Functional annotation of the M. japonicus and M. pulchricaudatus transcriptomes

For the functional annotation, the entire unigenes sets of the two transcriptomes were searched using BLAST (*E*-value $< 1e^{-5}$) against priority-ordered protein databases (Nr, Swiss-Prot, Pfam, KEGG, COG, GO) (Table 2). Based on the Nr and Pfam annotations, all-unigenes were assigned Gene Ontology (GO) terms using Blast2GO v2.5. A total of 19936 (25.87%) unigenes for *M. japonicus* and 19403 (22.94%) unigenes for *M. pulchricaudatus* were classified into three main GO categories comprising 59 groups (Fig. S3). For both species, the gene function distributions were extremely similar. In the three main categories (biological process, molecular function and cellular component), the 'cellular process' (54.8% and 54.9% for *M. japonicus* and *M. pulchricaudatus*, respectively), 'binding' (51.6% vs 51.5%) and 'cell' (32.5% vs 32.4%) terms were prominent (Fig. S3). In the KOG analysis, 8907 and 7950 annotated genes from *M. japonicus* and *M.*

Table 2
Annotation of the results of the *M. japonicus* and *M. pulchricaudatus* transcriptome comparison.

		M. japonicus		*M. pulchricaudatus*	
		Number	Percentage	Number	Percentage
Functional annotations	NR	18549	24.07%	14479	17.12%
	NT	6341	8.22%	6634	7.84%
	KEGG	9741	12.64%	9035	10.68%
	SwissProt	15176	19.69%	14345	16.96%
	PFAM	19649	25.5%	19170	22.67%
	GO	19936	25.87%	19403	22.94%
	KOG	8907	11.56%	7950	9.4%
	All Databases	2383	3.09%	1859	2.19%
	At least one Database	26213	34.02%	25296	29.91%
CDS annotations	Homolog	14126	18.33%	13695	16.2%
	ESTSCAN	31234	40.54%	33389	39.49%
	All	45360	58.87%	47084	55.68%

pulchricaudatus, respectively, were classified into 26 functional categories (Fig. S4). Among these categories, the unigenes in the "translation, ribosomal structure and biogenesis" category between the species showed a relatively high difference, based on percent (9.15% vs 6.03%), followed by the terms "general function prediction only" (13.77% vs 14.29%) and "posttranslational modification, protein turnover, chaperones" (10.94% vs 10.27%). The KEGG database was used to further predict metabolic pathways. A total of 15552 (20.2%) unigenes for *M. japonicus* and 13932 (16.5%) unigenes for *M. pulchricaudatus* were assigned to 230 pathways (Fig. S5). Among these pathways, signal transduction-related pathways occupied the highest proportion (16.35% vs 16.8%), followed by endocrine system (9.04% vs 9.28%) and immune system (5.67% vs 5.84%).

3.3. Prediction of the coding sequences (CDS)

A total of 14126 and 13695 unigenes with CDS regions were extracted from *M. japonicus* and *M. pulchricaudatus*, respectively, based on the nr and Swiss-Prot protein database search (Table 2). In *M. japonicus*, 4400 (31.15%) CDSs were shorter than 500 bp, 3537 (25.04%) CDSs ranged from 500 to 1000 bp, and 6189 (43.81%) CDSs were longer than 1000 bp. In *M. pulchricaudatus*, 3846 (28.08%) CDSs were shorter than 500 bp, 3485 (25.45%) CDSs ranged from 500 to 1000 bp, and 6364 (46.47%) CDSs were longer than 1000 bp. There were 31234 (40.54%) and 33389 (39.49%) ORF-containing unigenes predicted by ESTScan (Table 2). According to the procedure of Wang et al., we obtained 13131 full-length CDS sequences in *M. japonicus* and 12607 full-length sequences in *M. pulchricaudatus*.

3.4. Identification of orthologous genes and Ka/Ks analysis

A total of 17045 pairs of orthologs were identified between *M. japonicus* and *M. pulchricaudatus*. Among these orthologous genes, 5036 pairs of single-copy orthologs were filtered. Using the PAML codeML package with default settings, the *Ka/Ks* ratios of 2491 pairs of orthologs were calculated (Fig. 1A). For these orthologous pairs, the mean values of *Ks*, *Ka* and *Ka/Ks* ratio were 0.019 ± 0.017, 0.002 ± 0.01 and 0.175 ± 0.632, respectively. The majority orthologs had *Ka/Ks* values less than 0.5 (91.5%, 2280/2491), indicating that these genes evolved under purifying selection. There were 49 ortholog pairs with a *Ka/Ks* ratio > 1 and 116 gene pairs had *Ka/Ks* value between 0.5 and 1, which were considered candidate genes that probably experienced adaptive evolution.

It is regarded as an effective method to estimate the divergence time between closely related species based on the peak of synonymous rates (*Ks*) [56,57]. In the study, the peak in the *Ks* value distribution was 0.0083 (Fig. 1B), which indicated the close genetic relationship between *M. japonicus* and *M. pulchricaudatus*. The average *Ks* rate in the nuclear genes of higher plants and mammals was probably 2×10^{-9}–8×10^{-9} substitutions per synonymous site per year [58,59]. Sharp et al. estimated that the substitution rate of nuclear genes in *Drosophila* was about three times higher than the average rate in mammals and a rate of 16×10^{-9} substitutions was suitable for *Drosophila* [60]. Based on the equation: T = K/2r [61], the divergence time between *M. japonicus* and *M. pulchricaudatus* is about 0.26–0.69 Mya.

3.5. Functional analysis of orthologous genes between two Marsupenaeus species

A detailed description of the 165 candidate orthologs with a *Ka/Ks* ratio > 0.5 is provided in Table S2. The positively selected orthologous genes related to the immune process mainly comprised single *VWC* domain protein, *legumain*, *ras-related C3* botulinum, *caspase*, profilin family protein, *Ras*, and *C-type lectin*. These genes were mainly annotated with the GO terms molecular function (kinase regulator activity, protein serine/threonine kinase inhibitor activity), biological process (innate immune response, immune system process and response to stress), and cellular component (peroxisome and peroxisomal membrane). Based on the KEGG pathway analyses, these orthologs were involved in a variety of immune functions (toll-like receptor signaling pathway, natural killer cell mediated cytotoxicity and PI3k-akt signaling pathway), and hypoxia signaling (HIF-1 signaling pathway and VEGF signaling pathway). The top 20 statistically significant KEGG pathways are shown in Fig. 2.

3.6. Hypoxia tolerance related genes

Hypoxia inducible factor (HIF) is an oxygen-dependent transcription factor that regulates hypoxia-responsive genes expression by binding their HRE (hypoxia responsive element) sequences [62,63]. The comparison of the *HIF-1α* protein sequences revealed that two hydrophilic serine sites in the *M. japonicus* sequence were replaced, respectively, by a hydrophobic glycine and leucine in *M. pulchricaudatus* (Fig. S6A). *HIF-1α*, *HK*, *PFK*, *Hsp70* and *Hsp90* had a higher expression in *M. pulchricaudatus* than in *M. japonicus* based on the *EF1-alpha* gene (Fig. 3). In this study, mitogen-activated protein kinase (*MEK*) had a *Ka/Ks* > 1 (Table S2); *MEK* plays a key role in the expression of the *HIF-1α* gene [64].

M. pulchricaudatus are mainly distributed in lower latitudes and

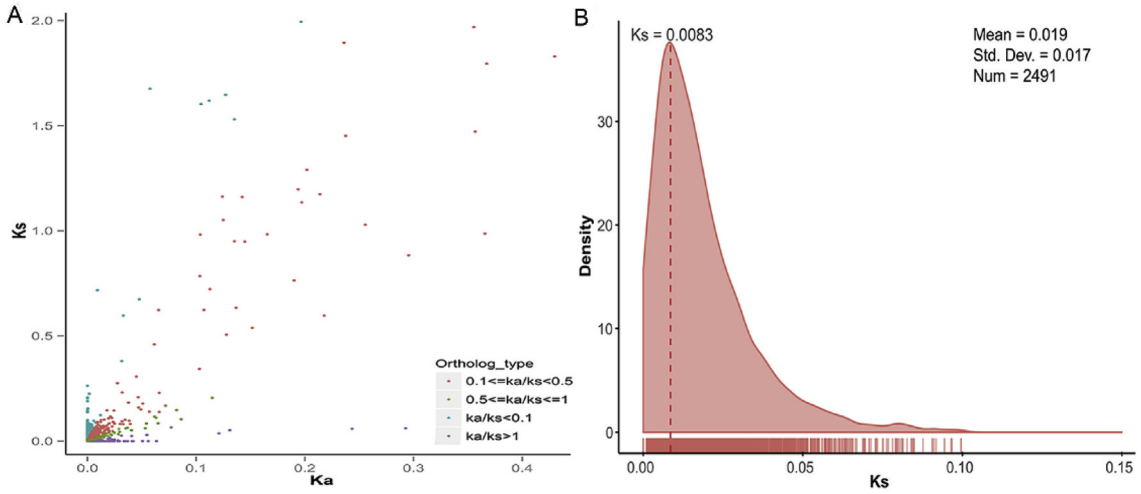

Fig. 1. Scatter plot distributions of *Ka/Ks* ratios and the *Ks* density distribution of orthologs between *M. japonicus* and *M. pulchricaudatus*.

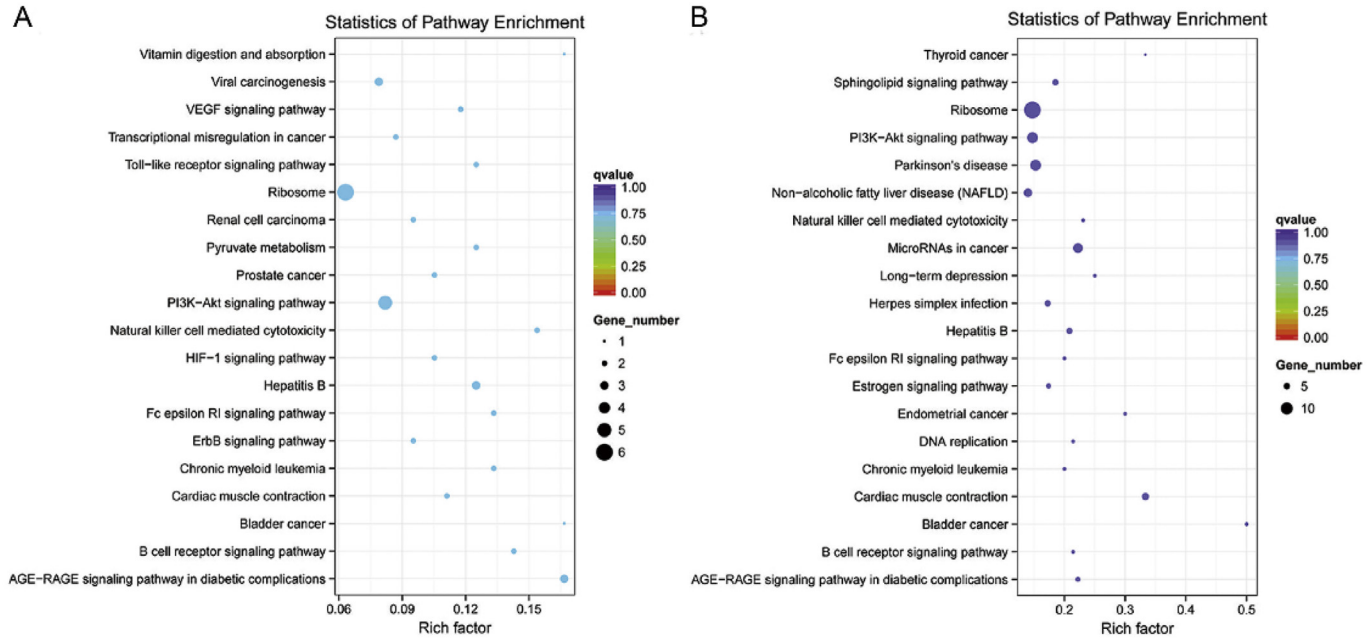

Fig. 2. The top 20 statistically significant KEGG classifications of candidate orthologs with *Ka/Ks* ratio > 1 (A) and between 0.5 and 1 (B).

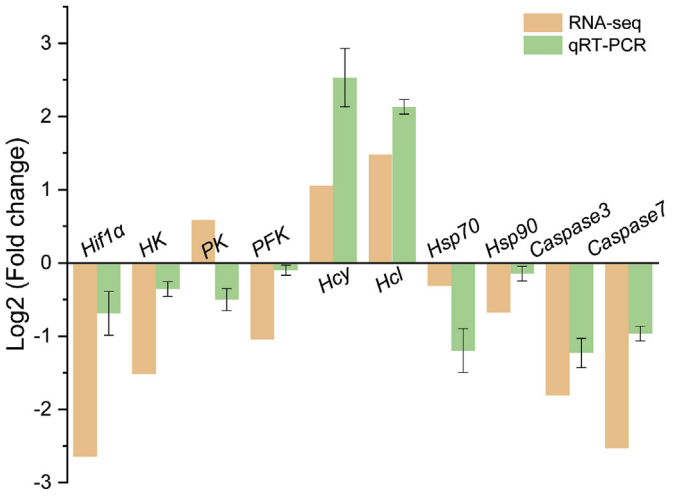

Fig. 3. Comparison of the expression profiles of ten unigenes determined by RNA-Seq and qRT-PCR.

experience higher annual temperatures; therefore, they have a higher heat tolerance than *M. japonicus*. The *Hcy* and *Hcl* had a higher expression in *M. japonicus* than in *M. pulchricaudatus* (Fig. 3). Comparison of the *Hcy* protein sequences revealed that the alanine and isoleucine of the *M. japonicus Hcy* were replaced, respectively, by proline and valine in *M. pulchricaudatus* (Fig. S6A). Based on sequence differences, the *AatII* (GACGT/C) restriction endonuclease was identified by DNAMAN 9.0 software and prospective products of endonuclease digestion were obtained from eight *M. pulchricaudatus* individuals (Fig. S6B). According to the alignment between our transcripts and hemocyanin sequences of *M. japonicus* (EF375712.1 and EF375711.1) and *Litopenaeus vannamei* (AJ250830.1), two mutational amino acid residues were located in the M domain, which responsible for oxygen transport.

3.7. Caspase gene family analysis

In this study, we found several caspase-like unigenes from two *Marsupenaeus* transcriptomes (Fig. 4), which have high consistency with the caspase genes of other animals. The Mj|c40522_g1 and Mp|c41538_g1 unigenes were matched with *Pjcaspase* (EF079670.1) and the orthologous gene pair had a *Ka/Ks* > 1.2 (Table S2). The comparison of the caspase protein sequences revealed that multiple amino acid variation sites were found between *M. japonicus* and *M. pulchricaudatus* (Fig. S6A). There was no transmembrane region and signal peptide by TMHMM Server 2.0 and SignalP 4.1 server, respectively. Using SOPMA method, the Mj|c40522_g1 and Mp|c41538_g1 protein sequences contained alpha helix (53.35%&54.92%), random coil (30.51%&29.72%), extended strand (11.22%&10.04%) and beta turn (4.92%&5.31%) (Fig. 5A). The caspase protein contained p10 (410–443), p20 subunits and CASc domain (240–495) (Fig. 5B), which was differ from typical caspase family. Moreover, the p20 subunits of two *Marsupenaeus* species had different length, 250–362 for *M. japonicus* and 260–362 for *M. pulchricaudatus*. The 3D structures of unigenes were predicted by the I-TASSER server (Fig. 5C). The template of the highest significance was *caspase*-7, which had a higher expression in *M. pulchricaudatus* than in *M. japonicus* (Fig. 3). Based on sequence differences, we identified the *Mfe I* (C/AATTG) restriction endonuclease by DNAMAN 9.0 software and obtained prospective products of endonuclease digestion from eight *M. pulchricaudatus* individuals (Fig. S6C).

3.8. Molecular phylogenetics of two Marsupenaeus species based on a single-copy gene

By pre-amplification, a fragment (1121bp) of the caspase gene was amplified. Based on the single copy *caspase* gene, eight populations of *Marsupenaeus* species were divided into two phylogeographic lineages from the East and South China (Fig. 6A). Genetic distance between populations ranged from 0.017 (HL2 & DD) to 0.038 (ZS & QG). The two *Marsupenaeus* species were divided into two clusters (Fig. 6B), *M. japonicus* (ZS, XP, XM and HL1) *and M. pulchricaudatus* (HL2, DD, ZH, QG and SY), which indicated the caspase gene could be used for phylogenetic analysis.

4. Discussion

Thus far, all studies about two related *Marsupenaeus* species have been based on morphology, mitochondrial DNA and ribosomal DNA. There was hardly any genetic information about *M. pulchricaudatus*. The

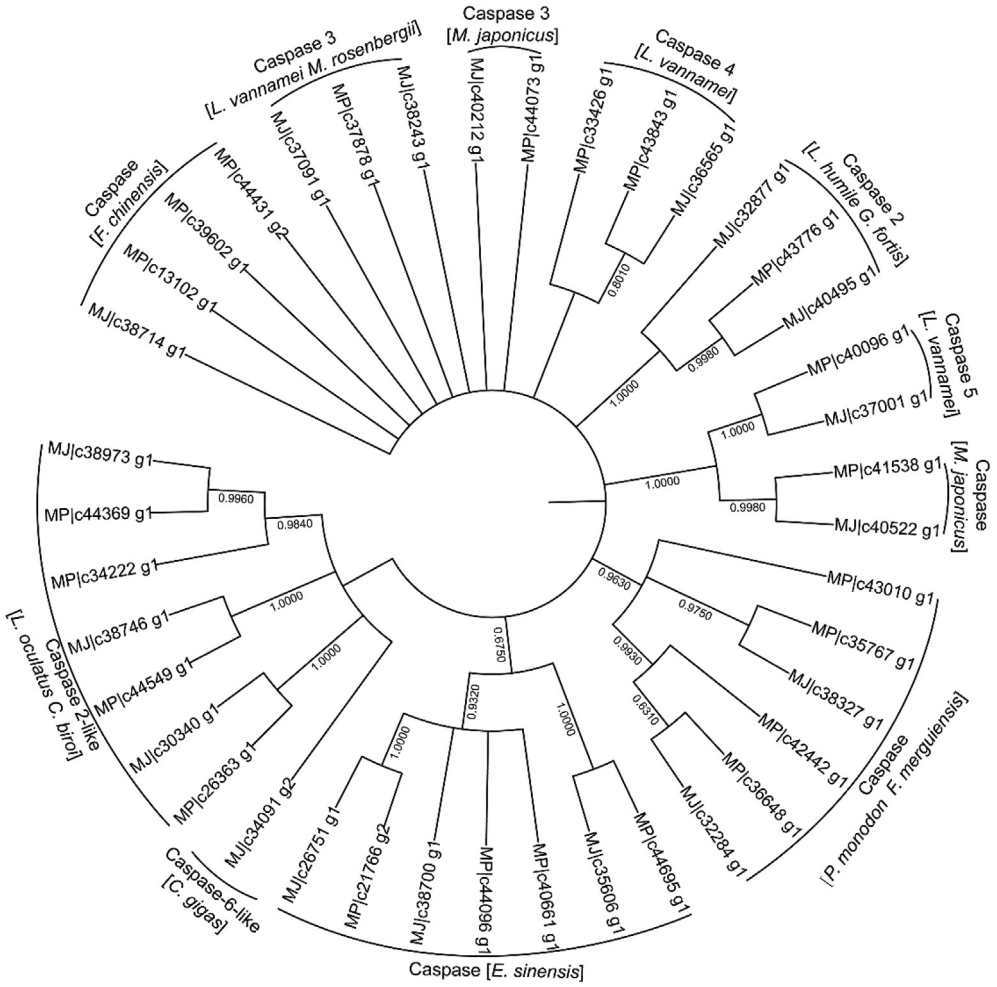

Fig. 4. Phylogenetic analysis of several caspase-like unigenes from two *Marsupenaeus* transcriptomes. *L. vannamei* = *Litopenaeus vannamei*, *F. chinensis* = *Fenneropenaeus chinensis*, *P. monodon* = *Penaeus monodon*, *F. merguiensis* = *Fenneropenaeus merguiensis*, *M. rosenbergii* = *Macrobrachium rosenbergii*, *L. humile* = *Linepithema humile*, *G. fortis* = *Geospiza fortis*, *E. sinensis* = *Eriocheir sinensis*, *C. gigas* = *Crassostrea gigas*, *L. oculatus* = *Lepisosteus oculatus*, *C. biroi* = *Cerapachys biroi*.

present study constitutes the first comparative analysis of the transcriptomes of two related *Marsupenaeus* species, which supplemented two *Marsupenaeus* species with genetic or genomic information.

In this study, we characterized and compared the comprehensive transcriptomes of two *Marsupenaeus* species, and obtained valuable genomic resources. Based on single-copy orthologous genes, hundreds of sequences experiencing adaptive evolution were identified, including 49 genes under strong positive selection. Those genes were predicted to be involved in immune functions and hypoxia signaling, which might contribute to the evolutionary differences between the two *Marsupenaeus* species. Based on the equation: T = K/2r, the divergence time between *M. japonicus* and *M. pulchricaudatus* is about 0.26–0.69 Mya, which was later than the evaluation time (1.1–4.7 Mya) from Tsoi et al. [5,6]. During the Middle Pleistocene, as sea levels fell by 100–150 m, the coastal areas along the South and East China Sea including Taiwan Strait were exposed [65]. This isolation mode greatly promotes species differentiation [66], which has been proved in *Oratosquilla oratoria* [67], *Bostrychus sinensis* [68,69], and *Lethrinid* fish [70].

Crustaceans mainly rely on the non-specific innate immunity, including physical defense, cellular and humoral immunity [71,72]. Caspases, the major players of apoptosis, is a family of structurally-related cysteine proteases and mainly contain inflammatory mediator (1,4,5,11), activator (2,8,9,10) and executioner (3,6,7) subfamilies. At present, only a few caspases have been found in prawn, such as *Pjcaspase* [23], *FcCasp* [73], *caspase-2* [74], and *Lvcaspase2-5* [75]. Among these, only a *Pj_caspase* gene was cloned for *M. japonicus*. In this study, we found several caspase-like unigenes, which would facilitate future studies on the molecular mechanism of apoptosis and invertebrate immunity. The *Pjcaspase* gene had been showed that it involved in apoptosis against WSSV infection [23], and the sequence diversity provided the molecular basis for the antiviral defense of shrimp [54]. *Caspase 2 and caspase 4* showed a significant upregulation in the *V. parahaemolyticus*-infected group [21,76]. In the study, the *caspase7* and *caspase3* (KX214529.1) had a higher expression in *M. pulchricaudatus* than in *M. japonicus* based on the *EF1-alpha* gene. As central effectors in apoptosis, different caspase genes have variant functions, which had been proved by Wongprasert [77] and Wang [75]. Obvious differences of three-dimensional and secondary structure may contribute to the functional differences.

The two *Marsupenaeus* species are distributed across different waters with varying temperatures. Compared with the high latitudes, the lower latitudes have higher annual temperatures, especially in the summer. When the dissolved oxygen changes, crustaceans raise their hemolymph pH or change the composition of Hc molecules to enhance hemocyanin oxygen affinity [78,79]. The amino acid changes in hemocyanin gene may affect oxygen transportation and help the two *Marsupenaeus* species better adapt to their habitat. Whether chronic hypoxia and higher annual temperatures have impact on the level of hemocyanin expression still needs further verification. Long-term hypoxia prompts

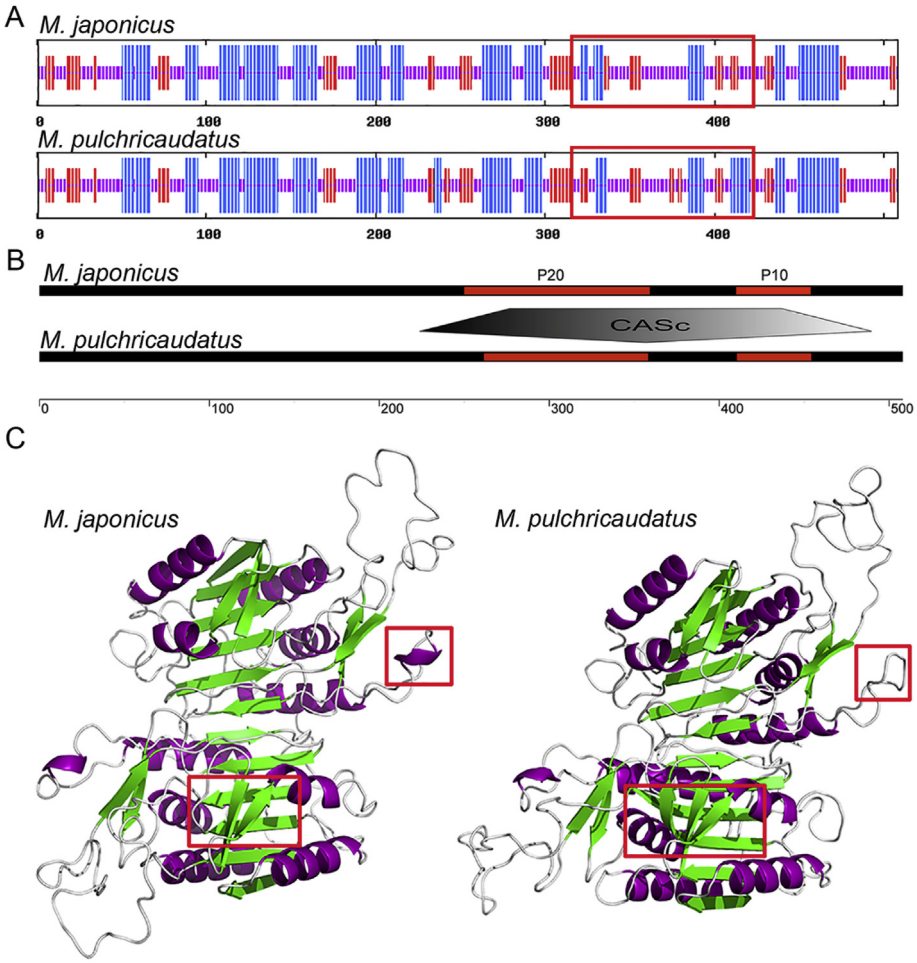

Fig. 5. The secondary and three-dimensional structure prediction of the Mj|c40522_g1 and Mp|c41538_g1 unigenes. (A) Predicted secondary structures (blue represent alpha helix and red represent extended strand), (B) structural domains and (C) 3D structures, the purple and green represent alpha-helices and beta-sheets, respectively. (For interpretation of the references to color in this figure legend, the reader is referred to the Web version of this article.)

crustaceans to initiate the synthesis mechanism of hemocyanin, which has been corroborated in *Callinectes sapidus*, *Nephrops norvegicus* and *Palaemonetes pugio* [80–82]. Song et al. discovered the thermotolerance of *M. pulchricaudatus* was stronger than that of *M. japonicus* by comparing the CTMax values and acclimation response ratio (ARR) values [16]. Our studies showed that *M. pulchricaudatus* had higher background expression levels of *Hsp70* and *Hsp90* than *M. japonicus*, which suggest that *M. pulchricaudatus* own a higher potential for stress defense. Heat shock protein 90, by binding to the *HIF-1α* PAS domain, prevents *HIF-1α* degradation by competing with *RACK1* (receptor for activated C-kinase 1) [83]. In addition, the *Hsp90* have an effect on the transcriptional activity [84] and nuclear translocation of *HIF-1α* [85]. In addition to regulating hypoxia-responsive genes, HIF-1 plays a crucial role in countering the oxidative injury and metabolic changes associated with WSSV infection [86,87].

Combining mitochondrial markers with nuclear genes, hybrid groups and hybrid abalone from interspecies hybridization were successfully identified [88,89]. The hemocyanin and caspase gene could be used to identify juvenile shrimp and hybridization of two *Marsupenaeus* species. The pooled hepatopancreas samples of Huilai populations were used for the transcriptome sequencing and qRT-PCR in this study. This strategy, to some degree, could reveal the differences in gene expression levels between two *Marsupenaeus* species. Nevertheless, the influence of various environmental factors should not be ignored. Thus, we will further verify these results through synchronous sampling from polyculture of two *Marsupenaeus* species in future studies.

For nuclear genes, the exon and intron sequences have different evolutionary rate, which suitable for studying middle-level phylogenetic relationships. The signal copy caspase gene was amplified successfully and used for phylogenetic analysis of two *Marsupenaeus* species. In accordance with previous studies [2,5,7], two *Marsupenaeus* species were divided into two clusters, *variety I* (ZS, XP, XM and HL1) *and variety II* (HL2, DD, ZH, QG and SY). Regier et al. sequenced 62 single-copy nuclear protein coding genes of 75 arthropod species and classified crustaceans into three categories [9]. Moreau et al. reconstructed the phylogeny of 139 extant genera based on six gene regions and deduced that the rise of angiosperms was related to herbivorous insects [90]. It is very controversial as to whether or not 29 *Penaeus* s.1. species should be split into six genera [91–93]. Developing more SCNGs helps reconstruct the phylogeny of *Penaeus* and provide new evidence for the classification of crustaceans.

In conclusion, this study provides abundant transcriptome resources and new insights into the evolutionary adaptation of immune defense and hypoxia tolerance in two closely related *Marsupenaeus* species. Moreover, this research will facilitate further comparative genomic studies of the two varieties.

Authors' contributions

PPW, YM conceived and designed the experiments. YM, YQS and JW obtained funds for the study. PPW and CFX performed molecular experiments and bioinformatics analysis. PPW and YM drafted the manuscript. YQS and JW participated in the manuscript revision. All authors read and approved the final manuscript.

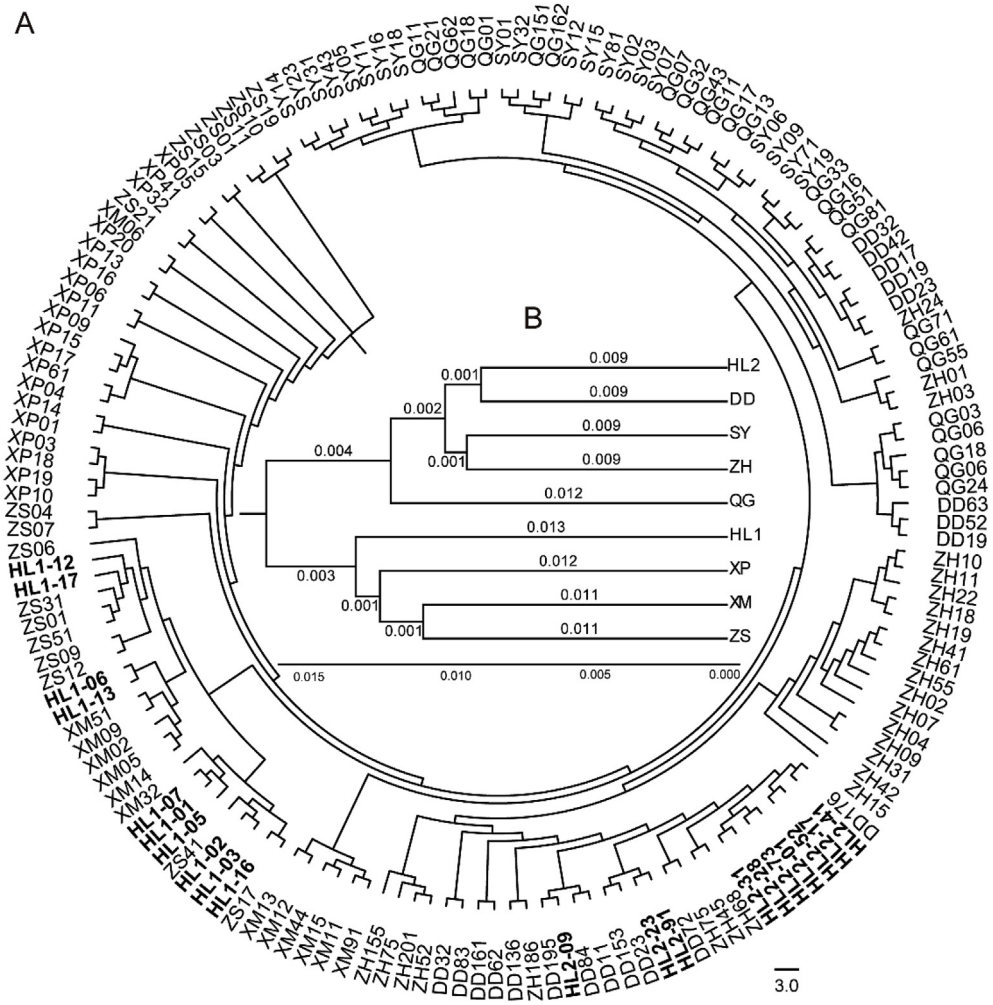

Fig. 6. Genetic structure of two *Marsupenaeus* species based on the single copy caspase gene. A total of 160 individuals were collected from eight localities in the southeast coast of China including Zhoushan (ZS), Xiapu (XP), Xiamen (XM), Huilai (HL), Zhuhai (ZH), Dongdi (DD), Qiaogang (QG) and Sanya (SY). (A) Neighbor joining (NJ) tree based on individual DNA sequences; (B) UPGMA clustering tree based on D_A genetic distance between populations.

Acknowledgments

This work was supported by the Project of China Agriculture Research System (Grant No. CARS-48), the Project of Fujian Provincial Department of Science and Technology (Grant No. 2016NZ0001-4), and Marine Economy Innovation and Development Project of Xiamen (Grant No. 16CZY009SF05). The authors declare no competing interests.

Appendix A. Supplementary data

Supplementary data to this article can be found online at https://doi.org/10.1016/j.fsi.2019.06.055.

References

[1] W. Dall, B.J. Hill, P.C. Rothlisberg, D.J. Sharples, The biology of the Penaeidae, J. Crustac Biol. 27 (6) (1990) 1–461.
[2] K.H. Tsoi, K.Y. Ma, T.H. Wu, S.T. Fennessy, K.H. Chu, T.Y. Chan, Verification of the cryptic species *Penaeus pulchricaudatus* in the commercially important kuruma shrimp *P. japonicus* (Decapoda : Penaeidae) using molecular taxonomy, Invertebr. Syst. 28 (5) (2014) 476.
[3] N.M. Tirmizi, *Marsupenaeus*, a new subgenus of *Penaeus Fabricius*, 1798 (Decapoda, Natantia), Pakistan J. Zool. 3 (2) (1971) 193–194.
[4] S. Lavery, T.Y. Chan, Y.K. Tam, K.H. Chu, Phylogenetic relationships and evolutionary history of the shrimp genus *Penaeus* s.l. derived from mitochondrial DNA, Mol. Phylogenetics Evol. 31 (1) (2004) 39–49.
[5] K.H. Tsoi, Z.Y. Wang, K.H. Chu, Genetic divergence between two morphologically similar varieties of the kuruma shrimp *Penaeus japonicus*, Mar. Biol. 147 (2) (2005) 367–379.
[6] K.H. Tsoi, T.Y. Chan, K.H. Chu, Molecular population structure of the kuruma shrimp *Penaeus japonicus* species complex in western Pacific, Mar. Biol. 150 (6) (2007) 1345–1364.
[7] Y.Q. He, Y.Q. Su, Y. Mao, J. Wang, Genetic diversity analysis of microsatellite DNA in different varieties of *Marsupenaneus japonicus*, J. Fish. China 36 (10) (2012) 1520–1528.
[8] D.E. Mccauley, M.F. Bailey, N.A. Sherman, M.Z. Darnell, J. Heredity, Evidence for paternal transmission and heteroplasmy in the mitochondrial genome of *Silene vulgaris*, a gynodioecious plant, Heredity 95 (1) (2005) 50–58.
[9] J.C. Regier, J.W. Shultz, Z. Andreas, H. April, B. Bernard, W. Regina, J.W. Martin, C.W. Cunningham, Arthropod relationships revealed by phylogenomic analysis of nuclear protein-coding sequences, Nature 463 (7284) (2010) 1079–1083.
[10] J.M. Duarte, P.K. Wall, P.P. Edger, L.L. Landherr, H. Ma, P.K. Pires, J. Leebens-Mack, C.W. dePamphilis, Identification of shared single copy nuclear genes in Arabidopsis, Populus, Vitis and Oryzaand their phylogenetic utility across various taxonomic levels, BMC Evol. Biol. 10 (1) (2010) 61.
[11] N.D. Jackson, B.C. Carstens, A.E. Morales, B.C. O'Meara, Species delimitation with gene flow, Syst. Biol. 66 (5) (2017) 799–812.
[12] J.F. Flot, Species delimitation's coming of age, Syst. Biol. 64 (6) (2015) 897–899.
[13] T.H. Struck, J.L. Feder, M. Bendiksby, S. Birkeland, J. Cerca, V.I. Gusarov, S. Kistenich, K.H. Larsson, L.H. Liow, M.D. Nowak, Finding evolutionary processes hidden in cryptic species, Trends Ecol. Evol. 33 (3) (2018) 153.
[14] R.L. Andrew, L. Bernatchez, A. Bonin, C.A. Buerkle, B.C. Carstens, B.C. Emerson, D. Garant, T. Giraud, N.C. Kane, S.M. Rogers, A road map for molecular ecology, Mol. Ecol. 22 (10) (2013) 2605–2626.
[15] H.B. Dong, Y.Q. Su, Y. Mao, L. Bian, J. Wang, Growth characteristics of two morphologically similar varieties of *Marsupenaeus japonicus* under indoor cultivation environment, J. Trop. Oceanogr. 33 (4) (2014) 51–60.
[16] X. Song, Y. Mao, H. Dong, M. Zhang, L. Bian, J. Wang, The thermotolerance of the two morphologically similar varieties of juvenile kuruma shrimp (*Marsupenaeus japonicus*), J. Fish. China 38 (1) (2014) 84–90.

[17] P.H. Wang, T. Huang, X. Zhang, J.G. He, Antiviral defense in shrimp: from innate immunity to viral infection, Antivir. Res. 108 (1) (2014) 129–141.

[18] T. Rőszer, The invertebrate midintestinal gland ("hepatopancreas") is an evolutionary forerunner in the integration of immunity and metabolism, Cell Tissue Res. 358 (3) (2014) 685–695.

[19] J. Zheng, M. Yong, Y. Su, J. Wang, Effects of nitrite stress on mRNA expression of antioxidant enzymes, immune-related genes and apoptosis-related proteins in *Marsupenaeus japonicus*, Fish Shellfish Immunol. 58 (2016) 239–252.

[20] X.W. Zhang, X.W. Wang, Y. Huang, K.M. Hui, Y.R. Shi, W. Wang, Q. Ren, Cloning and characterization of two different ficolins from the giant freshwater prawn *Macrobrachium rosenbergii*, Dev. Comp. Immunol. 44 (2) (2014) 359–369.

[21] X. Ren, P. Liu, J. Li, Comparative transcriptomic analysis of *Marsupenaeus japonicus* hepatopancreas in response to *Vibrio parahaemolyticus* and white spot syndrome virus, Fish Shellfish Immunol. 87 (2019) 755–764 https://doi.org/10.1016/j.fsi.2019.02.030.

[22] M. Tohru, K. Tomoya, Y. Terutoyo, S. Masahiro, I. Toshiaki, Identification of cDNA encoding Toll receptor, MjToll gene from kuruma shrimp, *Marsupenaeus japonicus*, Fish Shellfish Immunol. 24 (1) (2008) 122–133.

[23] L. Wang, B. Zhi, W. Wu, X. Zhang, Requirement for shrimp caspase in apoptosis against virus infection, Dev. Comp. Immunol. 32 (6) (2008) 706–715.

[24] K.K. Song, D.F. Li, M.C. Zhang, H.J. Yang, L.W. Ruan, X. Xun, Cloning and characterization of three novel WSSV recognizing lectins from shrimp *Marsupenaeus japonicus*, Fish Shellfish Immunol. 28 (4) (2010) 596–603.

[25] H.S. Jiang, W.M. Jia, X.F. Zhao, J.X. Wang, Four crustins involved in antibacterial responses in *Marsupenaeus japonicus*, Fish Shellfish Immunol. 43 (2) (2015) 387–395.

[26] S. Zhong, Y. Mao, J. Wang, M. Liu, M. Zhang, Y. Su, Transcriptome analysis of Kuruma shrimp (*Marsupenaeus japonicus*) hepatopancreas in response to white spot syndrome virus (WSSV) under experimental infection, Fish Shellfish Immunol. 70 (2017) 710–719.

[27] Y. Zhang, G. Gao, R. Lin, J.J. Aweya, M. Tao, F. Wang, Transcriptome analyses reveal *Litopenaeus vannamei* hemocytes response to lipopolysaccharide, Fish Shellfish Immunol. 76 (2018) 187–195.

[28] Z. Zheng, F. Wang, J.J. Aweya, R. Li, D. Yao, M. Zhong, S. Li, Y. Zhang, Comparative transcriptomic analysis of shrimp hemocytes in response to acute hepatopancreas necrosis disease (AHPND) causing *Vibrio parahemolyticus* infection, Fish Shellfish Immunol. 74 (2018) 10–18.

[29] D. Powell, W. Knibb, C. Remilton, A. Elizur, De-novo transcriptome analysis of the banana shrimp (*Fenneropenaeus merguiensis*) and identification of genes associated with reproduction and development, Mar. Genom. 22 (2015) 71–78.

[30] M.E. Hudson, Sequencing breakthroughs for genomic ecology and evolutionary biology, Mol. Ecol. Res. 8 (1) (2008) 3–17.

[31] L. Zhang, H.F. Yan, W. Wu, H. Yu, X.J. Ge, Comparative transcriptome analysis and marker development of two closely related *Primrose* species (*Primula poissonii* and *Primula wilsonii*), BMC Genomics 14 (1) (2013) 329-329.

[32] G. Li, Y. Zhao, S. Guo, B. Liu, Y. Chen, X. Sun, J. Feng, Comparative analysis of spleen transcriptome detects differences in evolutionary adaptation of immune defense functions in bighead carp and silver carp, Fish Shellfish Immunol. 84 (2018) 148–157.

[33] B.L. Lockwood, J.G. Sanders, G.N. Somero, Transcriptomic responses to heat stress in invasive and native blue mussels (genus *Mytilus*): molecular correlates of invasive success, J. Exp. Biol. 213 (20) (2010) 3548.

[34] X. Mu, G. Hou, H. Song, P. Xu, D. Luo, D. Gu, M. Xu, J. Luo, J. Zhang, Y. Hu, Transcriptome analysis between invasive *Pomacea canaliculata* and indigenous *Cipangopaludina cahayensis* reveals genomic divergence and diagnostic microsatellite/SSR markers, BMC Genet. 16 (1) (2015) 12.

[35] C. Nourisson, A. Muñoz-Merida, M. Carneiro, F.J.M.E.R. Sequeira, De novo transcriptome assembly and polymorphism detection in two highly divergent evolutionary units of Bosca's newt (*Lissotriton boscai*) endemic to the Iberian Peninsula, Mol. Ecol. Res. 17 (3) (2017) 546–549.

[36] I. Smolina, S. Kollias, E.F. Møller, P. Lindeque, A.Y.M. Sundaram, J.M.O. Fernandes, G. Hoarau, Contrasting transcriptome response to thermal stress in two key zooplankton species, *Calanus finmarchicus* and *C. glacialis*, Mar. Ecol. Prog. 534 (2015) 79–93.

[37] M.G. Grabherr, B.J. Haas, M. Yassour, J.Z. Levin, D.A. Thompson, I. Amit, X. Adiconis, L. Fan, R. Raychowdhury, Q. Zeng, Full-length transcriptome assembly from RNA-Seq data without a reference genome, Nat. Biotechnol. 29 (7) (2011) 644–652.

[38] R.D. Finn, P. Coggill, R.Y. Eberhardt, S.R. Eddy, J. Mistry, A.L. Mitchell, G.A. Salazar, The Pfam protein families database: towards a more sustainable future, Nucleic Acids Res. 44 (D1) (2015) D279–D285.

[39] S. Götz, J.M. Garcíagómez, J. Terol, T.D. Williams, S.H. Nagaraj, M.J. Nueda, M. Robles, M. Talón, J. Dopazo, A.J.N.A.R. Conesa, High-throughput functional annotation and data mining with the Blast2GO suite, Nucleic Acids Res. 36 (10) (2008) 3420–3435.

[40] Y. Moriya, M. Itoh, S. Okuda, A.C. Yoshizawa, M.J.N.A.R. Kanehisa, KAAS: an automatic genome annotation and pathway reconstruction server, Nucleic Acids Res. 35 (2007) 182–185.

[41] C. Iseli, C.V. Jongeneel, P. Bucher, ESTScan: a program for detecting, evaluating, and reconstructing potential coding regions in EST sequences, Proc. Int. Conf. Intell. Syst. Mol. Biol. 99 (2) (1999) 138–148.

[42] X.W. Wang, J.B. Luan, J.M. Li, Y.L. Su, J. Xia, S.S. Liu, Transcriptome analysis and comparison reveal divergence between two invasive whitefly cryptic species, BMC Genomics 12 (1) (2011) 458.

[43] L. Li, S.C. Jr, D.S. Roos, OrthoMCL: identification of ortholog groups for eukaryotic genomes, Genome Res. 13 (9) (2003) 2178–2189.

[44] J. Castresana, Selection of conserved blocks from multiple alignments for their use in phylogenetic analysis, Mol. Biol. Evol. 17 (4) (2000) 540–552.

[45] Z. Yang, PAML 4: phylogenetic analysis by maximum likelihood, Mol. Biol. Evol. 24 (8) (2007) 1586–1591.

[46] M.D. Young, M.J. Wakefield, G.K. Smyth, A.J.G.B. Oshlack, Gene ontology analysis for RNA-seq: accounting for selection bias, Genome Biol. 11 (2) (2010) R14-R14.

[47] X. Mao, T. Cai, J.G. Olyarchuk, L.J.B. Wei, Automated genome annotation and pathway identification using the KEGG Orthology (KO) as a controlled vocabulary, Bioinformatics 21 (19) (2005) 3787–3793.

[48] P. HO, K. R, Climate change affects marine fishes through the oxygen limitation of thermal tolerance, Science 315 (5808) (2007) 95–97.

[49] J.H. Zhang, Y. Zhang, B. Herman, Caspases, apoptosis and aging, Ageing Res. Rev. 2 (4) (2003) 357–366.

[50] C. Geourjon, G. Deléage, SOPMA: significant improvements in protein secondary structure prediction by consensus prediction from multiple alignments, Comput. Appl. Biosci. CABIOS 11 (6) (1995) 681–684.

[51] L. Ivica, D. Tobias, B. Peer, SMART 7: recent updates to the protein domain annotation resource, Nucleic Acids Res. 40 (Database issue) (2012) 302–305.

[52] C.J.A. Sigrist, C. Lorenzo, D.C. Edouard, P.S. Langendijk-Genevaux, B. Virginie, B. Amos, H. Nicolas, PROSITE, a protein domain database for functional characterization and annotation, Nucleic Acids Res. 38 (Database issue) (2010) D161.

[53] Y. Zhang, I-TASSER server for protein 3D structure prediction, BMC Bioinf. 9 (1) (2008) 40.

[54] B. Zhi, L. Wang, G. Wang, X. Zhang, Contribution of the caspase gene sequence diversification to the specifically antiviral defense in invertebrate, PLoS One 6 (9) (2011) e24955.

[55] S. Kumar, G. Stecher, M. Li, C. Knyaz, K.J.M.B. Tamura, X. Mega, Molecular evolutionary genetics analysis across computing platforms, Mol. Biol. Evol. 35 (6) (2018) 1547–1549.

[56] Y. Wang, J. Hey, Estimating divergence parameters with small samples from a large number of loci, Genetics 184 (2) (2010) 363–379.

[57] S.Q. Tao, B. Cao, C.M. Tian, Y.M. Liang, Comparative transcriptome analysis and identification of candidate effectors in two related rust species (*Gymnosporangium yamadae* and *Gymnosporangium asiaticum*), BMC Genomics 18 (1) (2017) 651.

[58] W.H. Li, M. Tanimura, P.M. Sharp, An evaluation of the molecular clock hypothesis using mammalian DNA sequences, J. Mol. Evol. 25 (4) (1987) 330–342.

[59] K.H. Wolfe, P.M. Sharp, W.H. Li, Rates of synonymous substitution in plant nuclear genes, J. Mol. Evol. 29 (3) (1989) 208–211.

[60] P.M. Sharp, W.H. Li, On the rate of DNA sequence evolution in *Drosophila*, J. Mol. Evol. 28 (5) (1989) 398–402.

[61] D. Graur, W. Li, Fundamentals of Molecular Evolution, second ed., Sinauer Associates, Sunderland, Massachusetts, 2000.

[62] G.L. Semenza, Regulation of mammalian O2 homeostasis by hypoxia-inducible factor 1, Annu. Rev. Cell Dev. Biol. 15 (15) (1999) 551–578.

[63] J.W. Lee, S.H. Bae, J.W. Jeong, S.H. Kim, K.W. Kim, Hypoxia-inducible factor (HIF-1)alpha: its protein stability and biological functions, Exp. Mol. Med. 36 (1) (2004) 1–12.

[64] B. Emerling, L. Platanias, E. Black, A. Nebreda, R. Davis, N. Chandel, Mitochondrial reactive oxygen species activation of p38 mitogen-activated protein kinase is required for hypoxia signaling, Mol. Cell. Biol. 25 (12) (2005) 4853–4862.

[65] L. Wang, M. Sarnthein, H. Erlenkeuser, J. Grimalt, P. Grootes, S. Heilig, E. Ivanova, M. Kienast, C. Pelejero, U. Pflaumann, East asian monsoon climate during the late Pleistocene: high-resolution sediment records from the south China sea, Mar. Geol. 156 (1–4) (1999) 245–284.

[66] G. Ni, Q.I. Li, L. Kong, H. Yu, Comparative phylogeography in marginal seas of the northwestern Pacific, Mol. Ecol. 23 (3) (2014) 534–548.

[67] J. Cheng, Z.L. Sha, Cryptic diversity in the Japanese mantis shrimp *Oratosquilla oratoria* (Crustacea: squillidae): allopatric diversification, secondary contact and hybridization, Sci. Rep. 7 (1) (2017) 1972.

[68] F. Qiu, H. Li, H. Lin, S. Ding, M.M. Miyamoto, Phylogeography of the inshore fish, *Bostrychus sinensis* , along the Pacific coastline of China, Mol. Phylogenetics Evol. 96 (2016) 112–117.

[69] S. Ding, M. Mishra, H. Wu, S. Liang, M.M.J.H. Miyamoto, Characterization of hybridization within a secondary contact region of the inshore fish, *Bostrychus sinensis*, in the East China Sea, Heredity 120 (1) (2017) 51–62.

[70] A.J.E. Healey, N.J. Mckeown, A.L. Taylor, J. Provan, W. Sauer, G. Gouws, P.W. Shaw, Cryptic species and parallel genetic structuring in Lethrinid fish: implications for conservation and management in the southwest Indian Ocean, Ecol. Evol. 8 (4) (2018) 2182–2195.

[71] F. Li, J. Xiang, Recent advances in researches on the innate immunity of shrimp in China, Dev. Comp. Immunol. 39 (1–2) (2013) 11–26.

[72] I. Sadaaki, L. Bok Luel, Recent advances in the innate immunity of invertebrate animals, J. Biochem. Mol. Biol. 38 (2) (2005) 128–150.

[73] Y. Wang, J. Li, P. Liu, J. Li, Z. Zhang, Z. Chang, Y. He, D. Liu, The responsive expression of a caspase gene in Chinese shrimp *Fenneropenaeus chinensis* against pH stress, Aquacult. Res. 42 (8) (2011) 1214–1230.

[74] K. Deng, X. Shi, Y. Zhang, X. Meng, J. Kong, K. Luo, S. Luan, CDNA cloning of caspase2 gene in *Fenneropenaeus chinensis* and its expression analysis in WSSV infection, J. Fish. China 40 (1) (2016) 119–127.

[75] P.H. Wang, D.H. Wan, Y.G. Chen, S.P. Weng, X.Q. Yu, J.G. He, Characterization of four novel caspases from *Litopenaeus vannamei* (Lvcaspase2-5) and their role in WSSV infection through dsRNA-mediated gene silencing, PLoS One 8 (12) (2013) e80418.

[76] Z. Zheng, F. Wang, J.J. Aweya, R. Li, D. Yao, M. Zhong, S. Li, Y. Zhang, Comparative transcriptomic analysis of shrimp hemocytes in response to acute hepatopancreas necrosis disease (AHPND) causing *Vibrio parahemolyticus* infection, Fish Shellfish

Immunol. 74 (2017) 10–18.
[77] W. Kanokpan, S. Pakkakul, P. Amornrat, S. Saengchan, Cloning and characterization of a caspase gene from black tiger shrimp (*Penaeus monodon*)-infected with white spot syndrome virus (WSSV), J. Biotechnol. 131 (1) (2007) 9–19.
[78] N.M. Whiteley, E.W. Taylor, A.E. Haj, Seasonal and latitudinal adaptation to temperature in crustaceans, J. Therm. Biol. 22 (97) (1997) 419–427.
[79] G. Durstewitz, N.B. Terwilliger, Developmental changes in hemocyanin expression in the Dungeness crab, *Cancer magister*, J. Biol. Chem. 272 (7) (1997) 4347–4350.
[80] M. Brouwer, N.J. Brown-Peterson, P. Larkin, V. Patel, N. Denslow, S. Manning, Molecular and whole animal responses of grass shrimp, *Palaemone pugio*, exposed to chronic hypoxia, J. Exp. Mar. Biol. Ecol. 341 (1) (2007) 16–31.
[81] S. Baden, L. Pihl, R. Rosenberg, Effects of oxygen depletion on the ecology, blood physiology and fishery of the Norway lobster *Nephrops norvegicus*, Mar. Ecol. Prog. 67 (2) (1990) 141–155.
[82] J.G. Johnson, L.E. Burnett, K.G. Burnett, Uncovering hemocyanin subunit heterogeneity in *penaeid* shrimp using RNA-seq, Integr. Comp. Biol. 56 (6) (2016) 1080–1091.
[83] Y.V. Liu, J.H. Baek, H. Zhang, R. Diez, R.N. Cole, G.L. Semenza, RACK1 competes with HSP90 for binding to HIF-1α and is required for O2-independent and HSP90 inhibitor-induced degradation of HIF-1α, Mol. Cell 25 (26) (2007) 207–217.
[84] O. Alqawi, M. Moghaddas, G. Singh, Effects of geldanamycin on HIF-1alpha mediated angiogenesis and invasion in prostate cancer cells, Prostate Cancer Prostatic Dis. 9 (2) (2006) 126–135.
[85] D.M. Katschinski, L. Le, S.G. Schindler, T. Thomas, A.K. Voss, R.H. Wenger, Interaction of the PAS B domain with HSP90 accelerates hypoxia-inducible factor-1alpha stabilization, Cell. Physiol. Biochem. 14 (4–6) (2004) 351–360.
[86] M.M. Miranda-Cruz, J.J. Poom-Llamas, J.A. Godoy-Lugo, R.M. Ortiz, S. Gómez-Jiménez, J.A. Rosas-Rodríguez, E.F. Morán-Palacio, J.G. Soñanez-Organis, Silencing of HIF-1 in WSSV-infected white shrimp: effect on viral load and antioxidant enzymes, Comp. Biochem. Physiol. C Toxicol. Pharmacol. 213 (2018) 19–26.
[87] J.A. Godoy-Lugo, M.M. Miranda-Cruz, J.A. RosasRodríguez, N.P. Adan-Bante, J.G. Soñanez-Organis, Hypoxia inducible factor −1 regulates WSSV-induced glycolytic genes in the white shrimp *Litopenaeus vannamei*, Fish Shellfish Immunol. 92 (2019) 165–171.
[88] M. Qu, W. Tang, Q. Liu, D. Wang, S. Ding, Genetic diversity within grouper species and a method for interspecific hybrid identification using DNA barcoding and RYR3 marker, Mol. Phylogenetics Evol. 121 (2017) S1055790317305973.
[89] W. You, Q. Guo, C. Ke, P. Ren, X. Luo, M. Huang, A Two-step PCR Molecular Identification Method for Hybrid Progeny of *Haliotis fulgens* and *Haliotis Discushannai*, China, (2014) CN104004855B.
[90] C.S. Moreau, C.D. Bell, V. Roger, A.S. Bruce, N.E. Pierce, Phylogeny of the ants: diversification in the age of angiosperms, Science 312 (5770) (2006) 101–104.
[91] P.A. Mclaughlin, R. Lemaitre, F.D. Ferrari, D.L. Felder, R.T. Bauer, A reply to T.W. Flegel, Aquaculture 275 (1–4) (2008) 370–373.
[92] T.W. Flegel, Confirmation of the right to refuse revision in the genus *Penaeus*, Aquaculture 280 (1–4) (2008) 1–4.
[93] K.Y. Ma, T.Y. Chan, K.H. Chu, Refuting the six-genus classification of *Penaeus* s.l. (Dendrobranchiata, Penaeidae): a combined analysis of mitochondrial and nuclear genes, Zool. Scripta 40 (5) (2011) 498–508.